SUPPLEMENTARY INFORMATION

Precise delivery of a multifunctional nanosystem for MR-guided cancer therapy and monitoring of tumor response by functional diffusion-weighted MRI

Zeyu Xiao[a,#], Leung Chan[b,#], Dong Zhang[a,#], Cuiqing Huang[a], Chaoming Mei[b], Peng Gao[a], Yanyu Huang[b], Jianye Liang[a], Lizhen He[b], Changzheng Shi[a,c,*], Tianfeng Chen[b,*], Liangping Luo[a,*]

a: Medical Imaging Center, First Affiliated Hospital of Jinan University, Guangzhou, PR China

b: Department of Chemistry, Jinan University, Guangzhou, PR China

c: Department of Radiology, Johns Hopkins University School of Medicine, Baltimore, Maryland, USA.

Keywords: micelle, tumor targeting, theranostics, MRI, response evaluation

[#] ZY Xiao, L Chan and D Zhang contributed equally to this work.

[*] Corresponding authors: CZ Shi, TF Chen and LP Luo.

Results

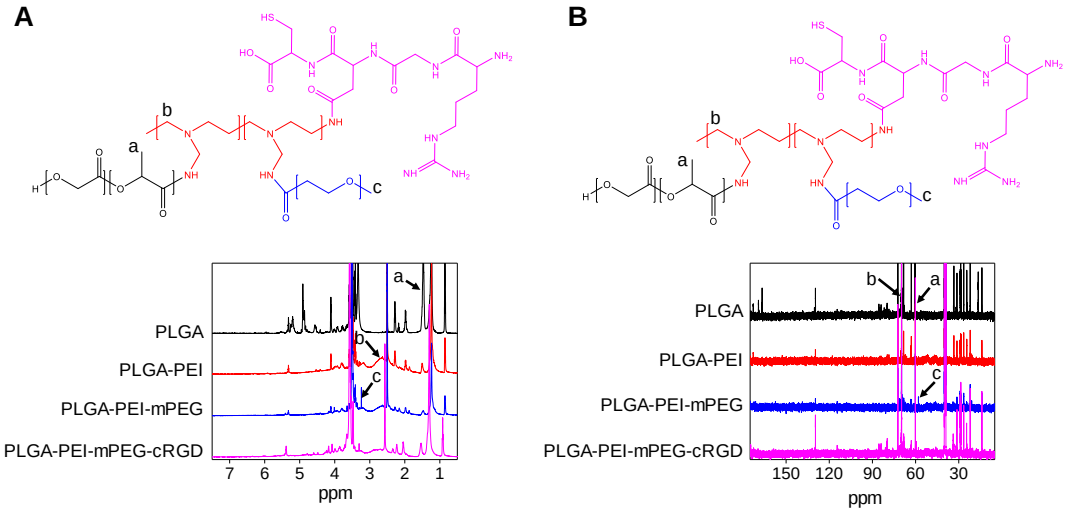

Aton	a	b	c
H (ppm)	1.23	2.64	3.23

Aton	a	b	c
C (ppm)	60	69	58.6

Figure S1. The chemical structures of the PLGA-PEI-mPEG-cRGD copolymers. The ^{1}H NMR and ^{13}C NMR spectra of PLGA, PLGA-PEI, PLGA-PEI-mPEG, and PLGA-PEI-mPEG-cRGD are shown. The chemical shifts of the characteristic H and C are shown in the tables.

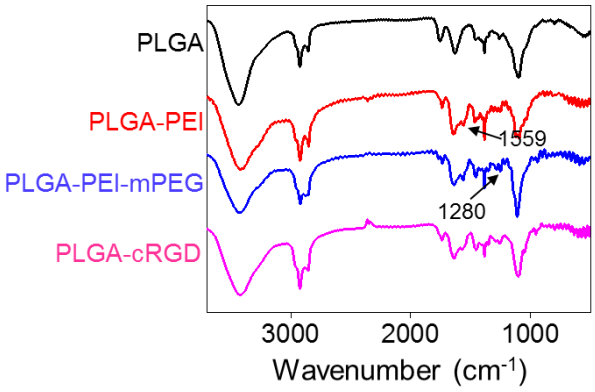

Figure S2. The FT-IR spectra of the PLGA, PLGA-PEI, PLGA-PEI-mPEG, and PLGA-cRGD copolymers. The black arrows indicate the amine group (1559 cm^{-1}) and the amide group (1280 cm^{-1}).

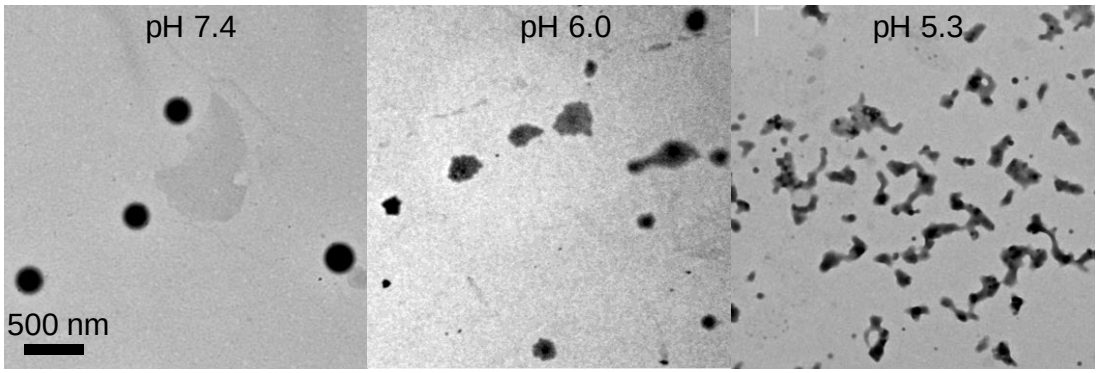

Figure S3. TEM images of cRGD-PLGA-SPIO@DOX nanoparticles under different pH conditions (pH = 7.4, 6.0 and 5.3).

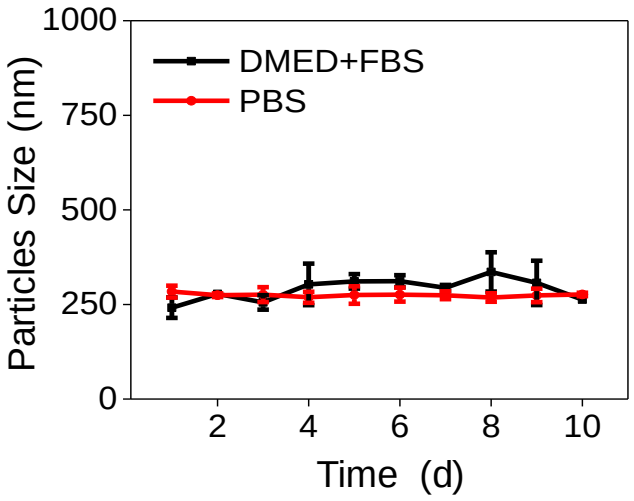

Figure S4. Change in particle size of the cRGD-PLGA-SPIO@DOX nanoparticles in DMEM+FBS and PBS solution for 10 days.

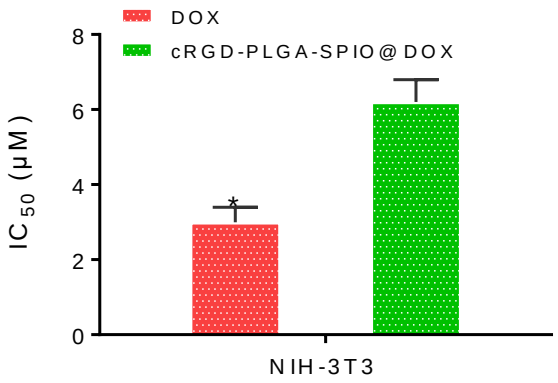

Figure S5. IC_{50} values for *in vitro* cytotoxicity against NIH-3T3 cancer cells. The averages and standard deviations from three experiments are shown.

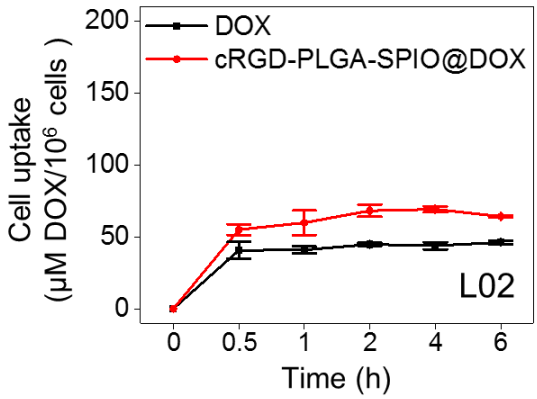

Figure S6. Quantitative analysis of cellular uptake of DOX and cRGD-PLGA-SPIO@DOX nanoparticles in L02 cells for 0.5, 1, 2, 4 and 6 h.

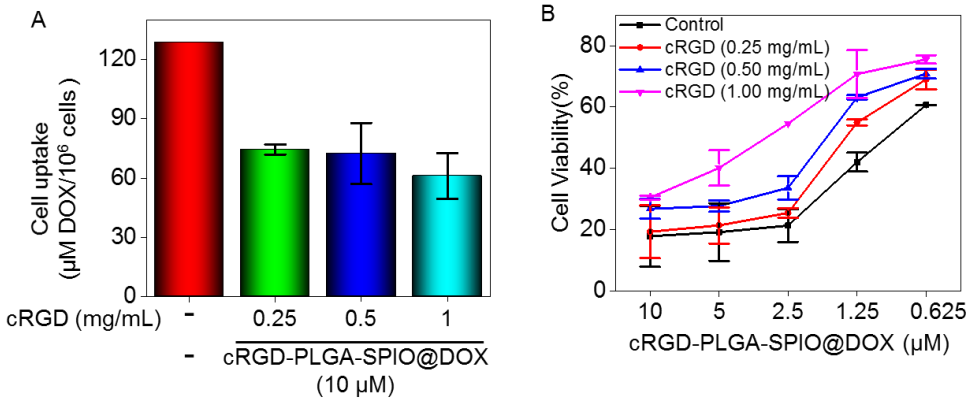

Figure S7. (A)The competition cellular uptake assay of cRGD-PLGA-SPIO@DOX nanoparticles. A549 cells were pretreated with 0.25, 0.5, or 1 mg/mL cRGD peptide and then treated with 10 μM cRGD-PLGA-SPIO@DOX nanoparticles for 6 h. (B) A549 cell viabilities in the competition uptake assays. A549 cells were pretreated with 0.25, 0.5, or 1.0 mg/mL cRGD peptide for 1 h, followed by incubation with 10, 5, 2.5, 1.25, or 0.625 μM cRGD-PLGA-SPIO@DOX nanoparticles for 72 h. The data are presented as the average ± standard deviation (n=3). Significant differences between the DOX and cRGD-PLGA-SPIO@DOX groups are indicated at the $P< 0.05$ (*) or $P< 0.01$ (**) level.

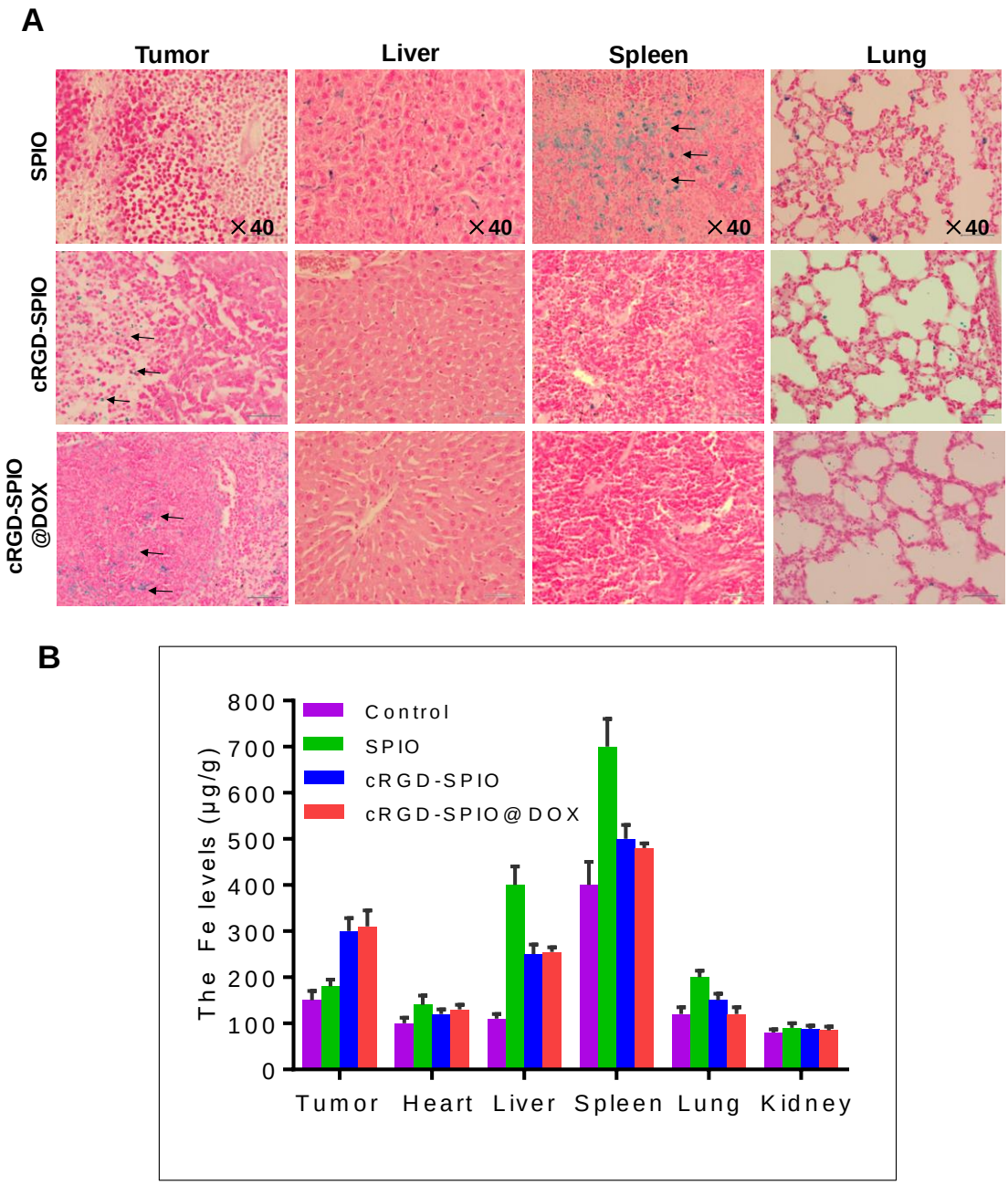

Figure S8. (A) Hematoxylin-eosin (H&E) and Prussian blue staining assays to verify Fe accumulation in the tumor, liver, spleen and lung. (B) Fe quantification in the tumor, liver, spleen and lung by ICP-MS in the control, SPIO, cRGD-SPIO, and cRGD-PLGA-SPIO@DOX groups.

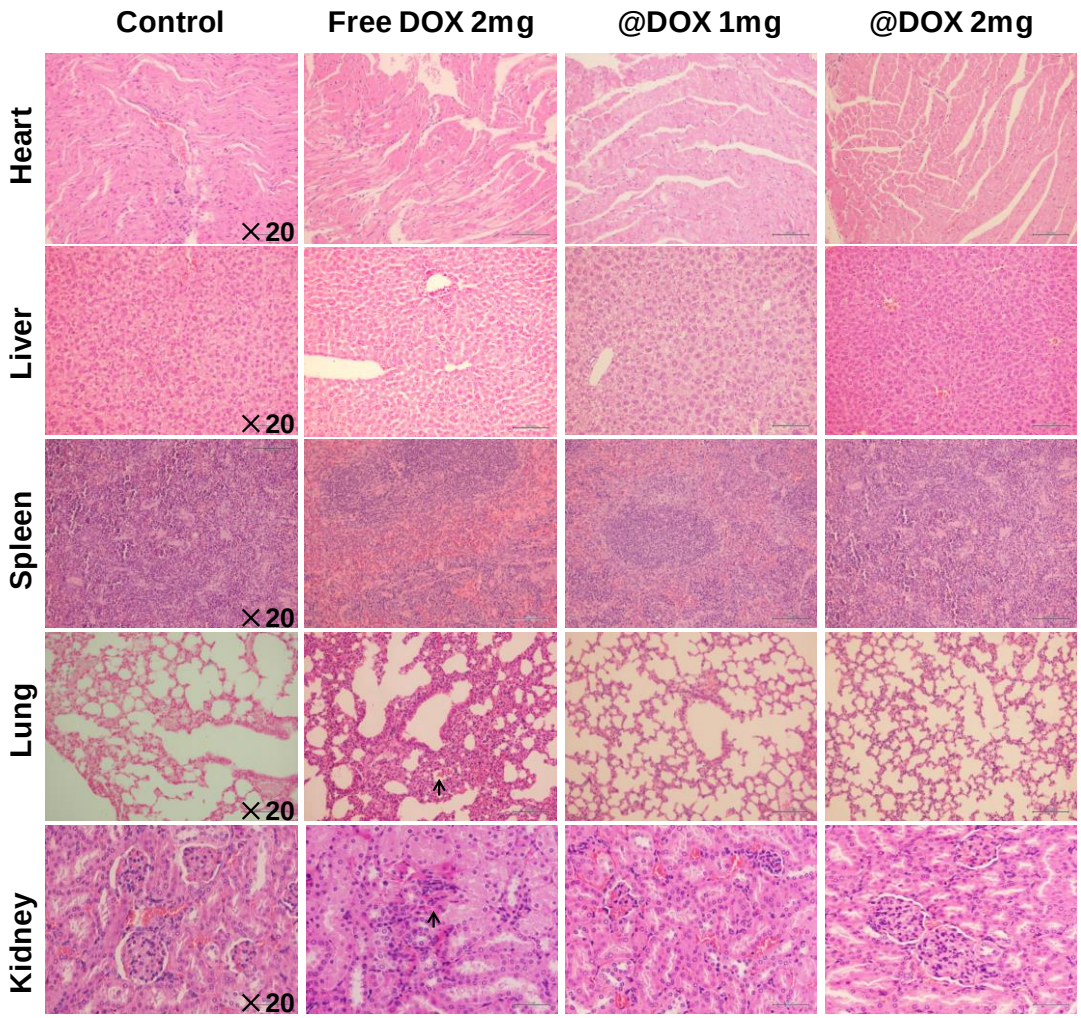

Figure S9. H&E-stained slice images of major organs (×20) from the DOX (2 mg/kg), cRGD-PLGA-SPIO@DOX (1 mg/kg), and cRGD-PLGA-SPIO@DOX (2 mg/kg) groups.

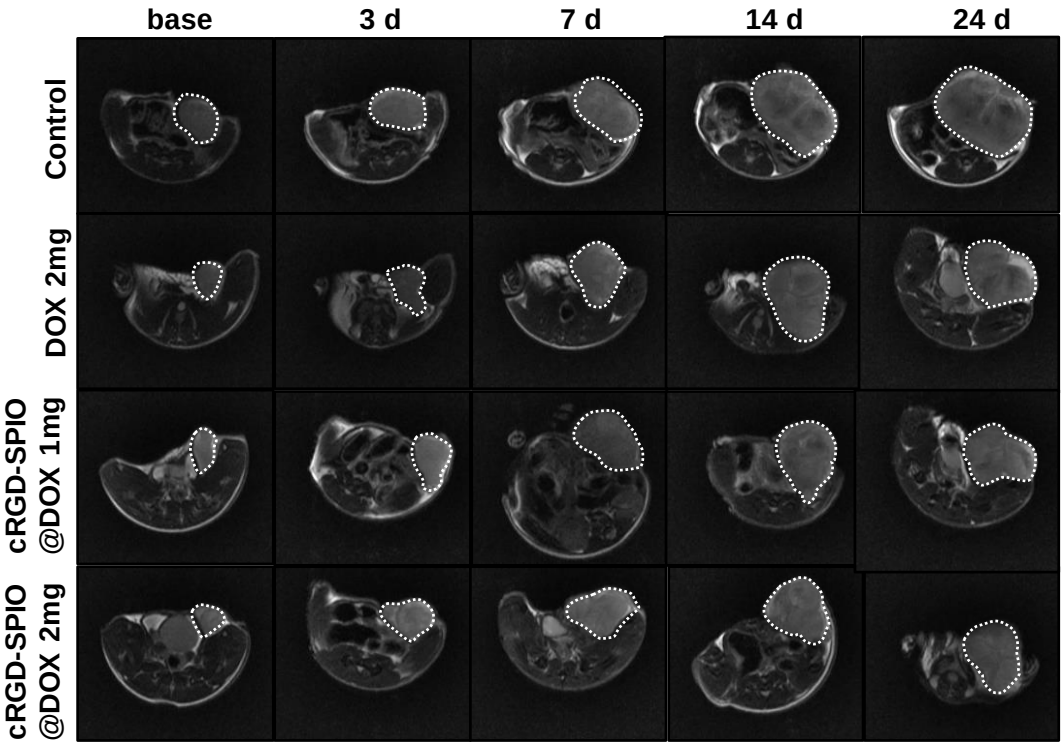

Figure S10. MR T_2WI anatomical images of representative Control, DOX and cRGD-PLGA-SPIO@DOX-treated tumors before and at different time points after treatment.